

# REVISITING THE CONFRONTATION OF THE SHOCK-POWERED SYNCHROTRON MASER MODEL WITH THE GALACTIC FRB 200428

YUN-WEI YU<sup>1,2</sup>, YUAN-CHUAN ZOU<sup>3</sup>, ZI-GAO DAI<sup>4</sup>, WEN-FEI YU<sup>5</sup>

*Draft version June 2, 2020*

## ABSTRACT

The recent discovery of a fast radio burst (FRB 200428) from the Galactic magnetar SGR 1935+2154 robustly indicated that FRB phenomena can sometimes be produced by magnetars, although it is uncertain whether the cosmological FRBs can share the same origin with this Galactic event. The association of FRB 200428 with an X-ray burst (XRB) further offers important implications for the physical processes responsible for the FRB phenomena. By assuming that the XRB emission is produced in the magnetosphere of the magnetar, we investigate the possibility that the FRB emission is produced by the synchrotron maser (SM) mechanism, which is powered by a shock due to the collision of an  $e^\pm$  ejecta with a baryonic cloud. It is found that this shock-powered SM model can in principle account for the FRB 200428 observations, if the collision just occurred on the line of sight and the ejecta launched by magnetar bursts can have appropriate ingredients and structures. To be specific, a burst ejecta should consist of an ultra-relativistic and extremely highly collimated  $e^\pm$  component and a sub-relativistic and wide-spreading baryonic component. The cloud blocking the  $e^\pm$  ejecta is just a remnant of a previous baryonic ejecta. Meanwhile, as a result of the synchrotron emission of the shocked material, an intense millisecond X-ray pulse is predicted to overlap the magnetosphere XRB emission, which in principle provides a way to test the model. Additionally, the peak frequency of the SM radiation is constrained to be about a few hundred MHz and the radiation efficiency is around  $10^{-4}$ .

*Subject headings:* stars: neutron — magnetar — radio continuum: general

## 1. INTRODUCTION

Fast radio bursts (FRBs) are mysterious radio transients, which were usually found at a typical observational frequency around  $\sim 1$  GHz and have fluences of a few to a few tens of Jy ms within a time interval of several milliseconds (Lorimer et al. 2007; Keane et al. 2012, 2016; Thornton et al. 2013; Burke-Spolaor & Bannister 2014; Spitler et al. 2014; Ravi et al. 2015; Masui et al. 2015; Champion et al. 2016; Caleb et al. 2017; Petroff et al. 2017; Bannister et al. 2017). The anomalously high dispersion measures (DMs) of FRBs at high Galactic latitudes usually indicate that these phenomena occurred at cosmological distances. According to the millisecond durations and high energy releases of FRBs, their origins are very likely to be related to the violent activities and even catastrophic collapses/coalescences of compact objects or binaries, in particular, of highly magnetized neutron stars (i.e., magnetars; Popov & Postnov 2010; Kulkarni et al. 2014; Katz 2016b; Connor et al. 2016; Cordes & Wasserman 2016; Lyutikov 2017). The magnetar activity model was also strongly supported by the discovery of repeating FRBs (e.g., FRB 121102) and a per-

sistent radio counterpart (Kashiyama & Murase 2017; Metzger et al. 2017; Cao et al. 2017b; Dai et al. 2017; Michilli et al. 2018).

Very recently, on 28 April 2020, both the CHIME/FRB and STARE2 instruments had surprisingly detected an FRB (FRB 200428) from the direction of a Galactic magnetar: SGR 1935+2154 (CHIME/FRB Collaboration 2020; Bochenek et al. 2020), while the magnetar had just been found to enter in an active state of X-ray bursts (XRBs) since half a month ago (Veres et al. 2020; Ridnaia et al. 2020a; Barthelmy et al. 2020). On the one hand, the DM of FRB 200428 was measured to be  $\sim 332.7$  pc cm $^{-3}$ . On the other hand, SGR 1935+2154 is potentially associated with a supernova remnant G57.2+0.8, which locates in the Outer arm of the Galaxy and has a distance in the range of 6.6 – 12.5 kpc (Kothes et al. 2018; Zhou et al. 2020; Zhong et al. 2020). The consistency between the DM of FRB 200428 and the distance of G57.2+0.8 strengthens the magnetar origin of this FRB.

Specifically, FRB 200428 has a double-peak structure with two components of a width of  $\Delta t_{\text{frb}} \sim 0.5$  ms and separated by  $\sim 28.91$  ms. The band-averaged fluences of the radio emission had been estimated to be 0.7 MJy ms and 1.5 MJy ms in the 400-800 MHz and the 1280-1530 MHz bands, respectively (CHIME/FRB Collaboration 2020; Bochenek et al. 2020). Meanwhile, among the detected XRBs, the one occurred at 2020-04-28 14:34:24 UTC was found to be temporally associated with the radio burst, after a correction of the dispersion between the X-ray and radio (CHIME/FRB Collaboration 2020; Li et al. 2020). This temporal association robustly suggests the intrinsic connection between the XRB and the FRB. The light curve of this XRB had been well

<sup>1</sup> Institute of Astrophysics, Central China Normal University, Wuhan 430079, China, yuyw@mail.ccnu.edu.cn

<sup>2</sup> Key Laboratory of Quark and Lepton Physics (Central China Normal University), Ministry of Education, Wuhan 430079, China

<sup>3</sup> School of Physics, Huazhong University of Science and Technology, Wuhan 430074, China

<sup>4</sup> School of Astronomy and Space Science, Nanjing University, Nanjing 210093, China

<sup>5</sup> Key Laboratory for Research in Galaxies and Cosmology, Shanghai Astronomical Observatory, Chinese Academy of Sciences, 80 Nandan Road, Shanghai 200030, China

recorded by the SuperAGILE and Anti-Coincidence detectors (Tavani et al. 2020), the Insight-HXMT (Li et al. 2020), the Konus-Wind (Ridnaia et al. 2020b), and the Integral (Mereghetti et al. 2020), which showed the XRB peaked about 0.5s after the trigger and has a duration about one second.

At present, it is almost certain that FRB 200428 originated from the activity of SGR 1935+2154. Then, it is necessary and interesting to investigate how can the magnetar activity lead to FRB emission. Some theoretical analyses/models have been suggested for understanding this unique FRB event (e.g., Margalit et al. 2020; Lu et al. 2020; Dai 2020). As usual, two coherent radiation mechanisms are involved including the curvature radiation and the synchrotron maser (SM) radiation, which have been previously investigated in many literature for cosmological FRBs (Kumar et al. 2017; Lu & Kumar 2018; Kumar & Lu 2020; Yang & Zhang 2018, 2020; Wang et al. 2019; Lyubarsky 2014; Lyutikov 2017; Beloborodov 2017; Waxman 2017; Ghisellini 2017; Long & Pe'er 2018; Plotnikov & Sironi 2019; Metzger et al. 2019). The focus of this Letter is on the SM mechanism powered by a relativistic shock, which could be in a debate in some works (e.g. Margalit et al. 2020; Lu et al. 2020). In Section 2, we briefly describe the observational features of FRB 200428 and its associated XRB. According to these, in Section 3 we carefully derive the observational constraints on the shock-powered SM model, which can provide a basis for judging the availability of the model. Finally, a conclusion and discussions are given in Section 4.

## 2. GENERAL PROPERTIES OF FRB 200428

First of all, by using a reference distance of  $d = 10$  kpc (Zhong et al. 2020), we can calculate the isotropically-equivalent energy releases of FRB 200428 in the STARE2 frequency range by

$$\mathcal{E}_{\text{frb}} = 4\pi d^2 F_\nu \Delta\nu = 4.5 \times 10^{34} \text{ erg}, \quad (1)$$

where the radio fluence  $F_\nu = 1.5$  MJy ms given by the STARE2 is used and the corresponding  $\Delta\nu = 250$  MHz. By contrast, the energy releases from cosmological FRBs were usually found to be around  $\sim 10^{38} - 10^{41}$  erg (without  $k$ -correction), which makes this Galactic FRB unique. Therefore, in principle, we cannot rule out that FRB 200428 could be intrinsically different from the cosmological ones.

Meanwhile, the average luminosity of FRB 200428 can be calculated by

$$\mathcal{L}_{\text{frb}} = 4\pi d^2 S_\nu \Delta\nu = 7.5 \times 10^{37} \text{ erg s}^{-1}, \quad (2)$$

with  $S_\nu = 2.5$  MJy (Bochenek et al. 2020). This luminosity can be enhanced more, if a wider energy band is taken into account. In comparison, the spin-down luminosity of the magnetar can be estimated by

$$\mathcal{L}_{\text{sd}} = \frac{B_p^2 R_s^6 \Omega^4}{6c^3} = 1.4 \times 10^{34} \text{ erg s}^{-1}, \quad (3)$$

where  $B_p = 4.0 \times 10^{14}$  G,  $R_s \approx 10$  km,  $\Omega = 2\pi/P$ , and  $P = 3.24$  s are the magnetic field strength, the radius, the spin frequency, and the spin period of the magnetar, respectively (Israel et al. 2016). It is showed that,

unless the FRB emission is actually collimated within a solid angle smaller than one thousandth of  $4\pi$ , the spin-down power is not enough to drive the FRB emission. From this point of view, some related FRB models such as the giant pulse model (Connor et al. 2016; Cordes & Wasserman 2016; Lyutikov 2017) could be disfavored. Alternatively, FRB 200428 is very likely to be powered by the engine responsible for the associated XRB, in view of the huge energy release during the XRB as

$$\mathcal{E}_X = 4\pi d^2 F_X = 8.6 \times 10^{39} \text{ erg}. \quad (4)$$

Here, the unabsorbed fluence of the XRB in the 1-250 keV band is taken as  $(7.17^{+0.41}_{-0.38}) \times 10^{-7}$  erg/cm<sup>2</sup> (Li et al. 2020).

The brightness temperature of FRB 200428 at  $\nu \sim 1.4$  GHz can be preliminarily estimated by

$$T_{\text{B}, 1.4\text{GHz}} = \frac{c^2}{2k_B \nu^2} \frac{S_\nu d^2}{\Sigma} \sim 10^{31} \text{ K}, \quad (5)$$

where the area of emitting region is estimated by  $\Sigma = 4\pi(c\Delta t_{\text{frb}})^2$  with  $\Delta t_{\text{frb}} \sim 0.5$  ms. This result is much lower than those of the cosmological FRBs but still requires coherent radiation. Therefore, the radio emission must not be the extension of the XRB emission. Instead, it could be another consequence of the magnetar burst in addition to the XRB emission. As a natural consideration, a relativistic ejecta could be driven by the magnetar burst and be shot into the wind region of the magnetar. Then, in principle, it is possible to drive SM radiation by the ejecta, if the ejecta can collide with a magnetized plasma previously existing in the magnetar surroundings.

## 3. THE MODEL AND OBSERVATIONAL CONSTRAINTS

### 3.1. The radiation radius and burst ejecta properties

It is usually suggested that SM radiation can be powered by a relativistic shock propagating into a moderately magnetized ( $\sigma > 10^{-3}$ ) medium (Lyubarsky 2014; Beloborodov 2017; Metzger et al. 2019). The charges entering the shock gyrate around the ordered magnetic field and then the shock is mediated by the Larmor rotation of the charge. In the magnetar activity model, such a shock can arise from a collision of an ultra-relativistic ejecta with ambient medium. More specifically, the ejecta, which probably consists of electron-positron pairs, can be driven by the engine that triggers the XRB. The ambient medium could either be the magnetar wind nebula (Lyubarsky 2014) or a baryon-loaded cloud existing in the magnetar wind (Metzger et al. 2019).

By considering that the XRB associated with FRB 200428 is not intrinsically different from the other XRBs of the magnetar, it is assumed to occur in the magnetosphere. In this case, the causality between the XRB and the FRB can be connected by the motion of the  $e^\pm$  ejecta from the magnetosphere to the ambient medium at the radius of  $R_{\text{frb}}$ . This catch-up process leads to an intrinsic time delay for the radio emission relative to the XRB as

$$t_{\text{del}} = \frac{R_{\text{frb}}}{v_\pm} \left( 1 - \frac{v_\pm}{c} \cos \theta_v \right), \quad (6)$$

where  $v_\pm$  is the velocity of the  $e^\pm$  ejecta and  $\theta_v$  is the viewing angle between the velocity direction

and the line of sight (LOS). The observation of FRB 200428 and its associated XRB shows that this intrinsic time delay cannot be longer than a few millisecond (CHIME/FRB Collaboration 2020; Li et al. 2020). In this case, Equation (6) indicates the motion of the ejecta must be ultra-relativistic of a Lorentz factor  $\Gamma_{\pm}$  and the angle  $\theta_v$  should be smaller than  $1/\Gamma_{\pm}$ . Therefore, we can get

$$R_{\text{frb}} = 2\Gamma_{\pm}^2 ct_{\text{del}} = 6.0 \times 10^{14} \Gamma_{\pm,3.5}^2 t_{\text{del},-3\text{cm}}. \quad (7)$$

Then, it is demonstrated that the ambient medium blocking the  $e^{\pm}$  ejecta cannot be the magnetar wind nebula. Instead, it is probably a baryonic cloud, which could be a remnant of the previous burst ejecta. Therefore, as a complete understanding, the ejecta driven by a magnetar burst should consist of an ultra-relativistic  $e^{\pm}$  component and a sub-relativistic baryonic component. The baryonic component could be erupted by the burst from the magnetar crust. Because of their different origins and ingredients, these two components probably have different magnetizations and different durations. It is suggested that the highly magnetized  $e^{\pm}$  ejecta can only be produced during the peak of the burst energy release with a millisecond duration, whereas the baryonic ejecta can last for the whole burst period of a few seconds.

Violent bursts can frequently happen in the whole life of the magnetar and, in particular, intensively in an active state. So, it is expected that many baryonic ejecta can be distributed in the magnetar wind at different radius and different directions, as illustrated in Figure 1.

### 3.2. Parameter constraints

According to Equation (6), the XRBs of magnetars can be temporally associated by a radio burst, only if an ion-electron plasma cloud has exist in the moving direction of the new-launched  $e^{\pm}$  ejecta. Furthermore, the collision should happen on the LOS. The pre-existing cloud can be erupted by the magnetar earlier than the FRB event by an advance time of  $t_a \sim R_{\text{frb}}/v_{\text{ej},B}$ , where  $v_{\text{ej},B}$  is the velocity of the cloud (i.e., the baryonic component of the previous ejecta). Please notice that the advance time involved here is not the waiting time between two successive bursts. By considering of the month-long duration of the magnetar activity, we assume the advance time to be on the order of a few days. Then, the relationship between the velocities of the two ejecta components can be written as

$$\Gamma_{\pm,3.5}^{-2} v_{\text{ej},B,9.5} = 1.9 t_{\text{del},-3} t_{a,5}^{-1}. \quad (8)$$

When an  $e^{\pm}$  ejecta collides with an ion-electron cloud, a pair of shocks can in principle be driven. As suggested by Metzger et al. (2019), the FRB emission could be primarily contributed by the forward shock and the reverse shock contribution is nearly negligible, because of the different magnetizations of their upstream material. According to the numerical simulation by Plotnikov & Sironi (2019), we know that the peak frequency  $\nu_{\text{pk}}$  of a SM spectrum powered by the forward shock is about  $3\Gamma$  times of the plasma frequency of the cloud material  $\nu_p = (n_c e^2 / \pi m_e)^{1/2}$  (Metzger et al. 2019), which  $\Gamma$  is the Lorentz factor of the shock. Therefore, the particle number density of the cloud can be

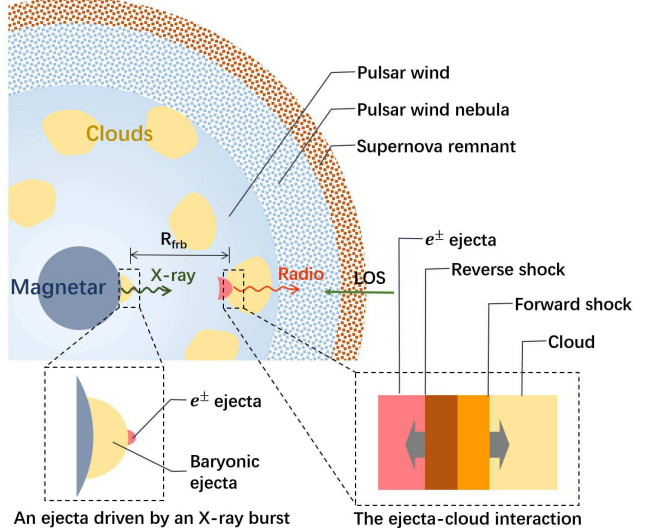


FIG. 1.— A cartoon illustration of FRB 200428 that arises from a shock-powered SM radiation at a radius of  $R_{\text{frb}}$ . Two shocks are driven by a collision of an ultra-relativistic  $e^{\pm}$  ejecta with an ion-electron plasma cloud, where the forward shock is responsible for the radio burst emission. The  $e^{\pm}$  ejecta is generated by the XRB temporally associated with FRB 200428, and the pre-existing cloud is just the ejecta remnant (the baryonic component) of a previous XRB.

estimated by

$$n_c = \frac{\pi m_e}{e^2} \left( \frac{\nu_{\text{pk}}}{3\Gamma} \right)^2 = 1.4 \times 10^6 \nu_{\text{pk},8.5}^2 \Gamma_1^{-2} \text{cm}^{-3}. \quad (9)$$

Then, according to the jump condition of the forward shock, the comoving energy density of the shocked cloud can be written as  $e'_{\text{sh}} = 4\Gamma^2 n_c m_p c^2$ , where the upstream material is considered to be magnetized for a degree of  $\sigma \sim 1$  and its influence on the jump condition is ignored for simplicity. Meanwhile, the kinetic energy flux carried by the  $e^{\pm}$  ejecta can be calculated by

$$L_{\pm} = \Gamma^2 e'_{\text{sh}} \Sigma_{\pm} c = 2.5 \times 10^{39} \nu_{\text{pk},8.5}^2 \Gamma_1^2 \Sigma_{\pm,21} \text{erg s}^{-1} \quad (10)$$

where  $\Sigma_{\pm}$  represents the cross section of the  $e^{\pm}$  ejecta. First of all, this kinetic energy flux is considered to be comparable to the XRB luminosity<sup>6</sup>, so the model parameters should satisfy

$$\nu_{\text{pk},8.5}^2 \Gamma_1^2 \Sigma_{\pm,21} \approx 4.0 \mathcal{L}_{X,40}. \quad (11)$$

Here, the length-scale of the ejecta cross section can be constrained to be about  $\sim 10^{10} - 10^{11}$  cm, which is much smaller than  $R_{\text{frb}} \sim 10^{14}$  cm. This indicates the  $e^{\pm}$  ejecta is a very narrow jet and even has a cylindric structure. In this case, the emission angle of the ejecta should be determined by  $1/\Gamma$  rather than by the opening angle of ejecta.

Therefore, on the one hand, the brightness tempera-

<sup>6</sup> It needs to be emphasized that we do not consider the  $e^{\pm}$  ejecta is a result of the XRB emission. Instead, the material ejection and the XRB are considered to be two separated consequences of a same explosive event with equipartition energies. Whereas the XRB emission is likely to be isotropic, the energy flux of the ejecta is highly collimated.

ture of the FRB should be re-estimated by

$$\begin{aligned} T_{\text{B},1.4\text{GHz}} &= \frac{c^2}{8\pi k_{\text{B}}\nu^2} \frac{\mathcal{L}_{\text{frb}}}{\Delta\nu\Gamma^2\Sigma_{\pm}} \\ &= 5.3 \times 10^{22} \mathcal{L}_{\text{frb},37} \Gamma_1^{-2} \Sigma_{\pm,21}^{-1} \text{K}. \end{aligned} \quad (12)$$

The radio burst emission can penetrate the cloud, only if the optical depth due to the induced Compton scattering is smaller than  $\sim 3$ , which can be determined as (Lyubarsky & Ostrovska 2016; Metzger et al. 2019)

$$\begin{aligned} \tau_{\text{ic},1.4\text{GHz}} &= \frac{1}{10} \frac{k_{\text{B}}T_{\text{B}}}{m_{\text{e}}c^2} \sigma_{\text{T}} n_{\text{c}} c \Delta t_{\text{frb}} \\ &= 24.5 \mathcal{L}_{\text{frb},37} \Delta t_{\text{frb},-3} \nu_{\text{pk},8.5}^2 \Gamma_1^{-4} \Sigma_{\pm,21}^{-1}. \end{aligned} \quad (13)$$

Then the second constraint on the model parameters can be yielded to

$$\nu_{\text{pk},8.5}^{-2} \Gamma_1^4 \Sigma_{\pm,21} \approx 8.2 \mathcal{L}_{\text{frb},37} \Delta t_{\text{frb},-3}. \quad (14)$$

On the other hand, if we tentatively take an index of  $-2$  for the  $L_{\nu}$  spectrum above the peak frequency, then the FRB luminosity can be corrected from the isotropically-equivalent observational one to

$$\begin{aligned} L_{\text{frb,cor}} &\approx \nu_{\text{pk}} \frac{\mathcal{L}_{\text{frb}}}{\Delta\nu\Gamma^2} \left( \frac{1.4\text{GHz}}{\nu_{\text{pk}}} \right)^2 \\ &= 2.5 \times 10^{36} \mathcal{L}_{\text{frb},37} \nu_{\text{pk},8.5}^{-1} \Gamma_1^{-2} \text{erg s}^{-1}. \end{aligned} \quad (15)$$

In comparison with the total energy flux of the  $e^{\pm}$  ejecta, the radiation efficiency of the SM can be constrained to

$$\xi \approx \frac{L_{\text{frb,cor}}}{L_{\pm}} \approx 1.0 \times 10^{-3} \mathcal{L}_{\text{frb},37} \nu_{\text{pk},8.5}^{-3} \Gamma_1^{-4} \Sigma_{\pm,21}^{-1}. \quad (16)$$

If we requires this radiation efficiency cannot be much higher than  $10^{-4}$  for an upstream magnetization of  $\sigma \sim 1.0$  (Plotnikov & Sironi 2019), then we can get the third constraint on the model parameters as

$$\nu_{\text{pk},8.5}^3 \Gamma_1^4 \Sigma_{\pm,21} \approx 10 \mathcal{L}_{\text{frb},37} \xi_{-4}^{-1}. \quad (17)$$

Here the primary uncertainty comes from the uncertain spectral index of the SM spectrum.

For a self-consistency between Equations (11), (14), and (17), we can finally obtain a plausible set of the model parameters as

$$\nu_{\text{pk}} \approx 3.3 \times 10^8 \Delta t_{\text{frb},-3}^{-1/5} \xi_{-4}^{-1/5} \text{Hz}, \quad (18)$$

$$\Gamma \approx 15.4 \mathcal{L}_{X,40}^{-1/2} \mathcal{L}_{\text{frb},37}^{1/2} \Delta t_{\text{frb},-3}^{1/10} \xi_{-4}^{-2/5}, \quad (19)$$

$$\Sigma_{\pm} \approx 1.6 \times 10^{21} \mathcal{L}_{X,40}^2 \mathcal{L}_{\text{frb},37}^{-1} \Delta t_{\text{frb},-3}^{1/5} \xi_{-4}^{6/5} \text{cm}^2, \quad (20)$$

which are directly dependent on the observational luminosities of the FRB and XRB and as well as the presumed SM radiation efficiency.

For the model parameters obtained above, we can derive a particle number flux of the  $e^{\pm}$  ejecta as

$$\begin{aligned} \dot{N}_{\pm} &= \frac{L_{\pm}}{(1 + \sigma_{\pm}) \Gamma_{\pm} m_{\text{e}} c^2} \\ &= 1.3 \times 10^{32} (1 + \sigma_{\pm})^{-1} \mathcal{L}_{X,40} \Gamma_{\pm,3.5}^{-1} \text{s}^{-1}, \end{aligned} \quad (21)$$

In principle, this can be explained by the Goldreich-Julian flux of the magnetar as  $N_{\text{GJ}} \sim \mu_{\pm} f_{\text{b}} R_{\text{L}}^2 n_{\text{GJ}} c \sim 10^{31} \mu_{\pm} f_{\text{b}} \text{s}^{-1}$ , if the magnetization of the flux  $\sigma_{\pm} \gg 1$ , the pair multiplicity  $\mu_{\pm} \gg 1$ , and the beaming factor of ejecta  $f_{\text{b}} \ll 1$  have appropriate values, where  $R_{\text{L}} = c/\Omega$  is the light cylinder radius and  $n_{\text{GJ}} = (\Omega B_{\text{p}}/2\pi ec)(R_{\text{L}}/R_{\text{s}})^{-3}$  is the Goldreich-Julian density. Furthermore, we can also make an estimation for the cloud properties. Firstly, the length-scale of the cloud in the longitude direction can be estimated by  $R_{\text{frb}}(r_{\text{b}}/R_{\text{s}})$ , where  $r_{\text{b}}$  is the radius of the region where the baryonic material erupted from on the magnetar surface. Secondly, the length-scale in the latitude direction can be determined by the ratio of the XRB duration ( $\Delta t_{\text{X}} \sim 1$  s) to the spin period ( $\sim 3$  s):  $\sim 2\pi R_{\text{frb}}/3$ . Finally, the thickness of the cloud is given by  $v_{\text{ej,B}} \Delta t_{\text{X}}$ . Following these considerations, the mass of the cloud and its kinetic energy can be calculated by

$$\begin{aligned} M_{\text{c}} &\approx \frac{4\pi r_{\text{b}}}{3R_{\text{s}}} R_{\text{frb}}^2 v_{\text{ej,B}} \Delta t_{\text{X}} n_{\text{c}} m_{\text{p}} \\ &= 5.0 \times 10^{20} \mathcal{L}_{X,40} \mathcal{L}_{\text{frb},37}^{-1} \Delta t_{\text{X},0} \Delta t_{\text{frb},-3}^{-3/5} t_{\text{del},-3}^2 \\ &\quad \xi_{-4}^{2/5} r_{\text{b},5} \Gamma_{\pm,3.5}^4 v_{\text{ej,B},9.5} \text{g}, \end{aligned} \quad (22)$$

and

$$\begin{aligned} E_{\text{ej,B}} &= \frac{1}{2} M_{\text{c}} v_{\text{ej,B}}^2 \\ &= 2.5 \times 10^{39} \mathcal{L}_{X,40} \mathcal{L}_{\text{frb},37}^{-1} \Delta t_{\text{X},0} \Delta t_{\text{frb},-3}^{-3/5} t_{\text{del},-3}^2 \\ &\quad \xi_{-4}^{2/5} r_{\text{b},5} \Gamma_{\pm,3.5}^4 v_{\text{ej,B},9.5}^3 \text{erg}, \end{aligned} \quad (23)$$

respectively. By assuming  $E_{\text{ej,B}} \approx \mathcal{E}_{\text{X}}$  and combining with Equation (8), we can get

$$\begin{aligned} \Gamma_{\pm} &\approx 2.9 \times 10^3 \mathcal{L}_{\text{frb},37}^{1/10} \Delta t_{\text{frb},-3}^{3/50} t_{\text{del},-3}^{-1/2} \\ &\quad \times \xi_{-4}^{-1/25} r_{\text{b},5}^{-1/10} t_{\text{a},5}^{3/10}, \end{aligned} \quad (24)$$

and

$$\begin{aligned} v_{\text{ej,B}} &\approx 5.4 \times 10^9 \mathcal{L}_{\text{frb},37}^{1/5} \Delta t_{\text{frb},-3}^{3/25} \\ &\quad \times \xi_{-4}^{-2/25} r_{\text{b},5}^{-1/5} t_{\text{a},5}^{-2/5} \text{cm s}^{-1}, \end{aligned} \quad (25)$$

which are very insensitive to the uncertain model parameters (i.e.,  $\xi$ ,  $r_{\text{b}}$ , and  $t_{\text{a}}$ ). As shown, the mass of the baryonic ejecta could be negligible in comparison to the total mass of a magnetar crust ( $\sim 10^{-5} M_{\odot}$ ) and thus the production of this baryonic ejecta is possible.

The self-consistent parameter constraints derived in this section suggest that the shock-powered SM model could in principle work for the observations of FRB 200428, if the ejecta has the appropriate ingredients and structures and the SM radiation has an appropriate efficiency.

### 3.3. Synchrotron emission

Besides the maser radiation, the shocked material can also release its internal energy through synchrotron emission, which then provides an extra counterpart for the FRB emission. As usual, the synchrotron emission can be characterized by the following two characteristic fre-

quencies

$$\begin{aligned}\nu_m &= \frac{3eB'_{sh}}{4\pi m_e c} \gamma_m^2 \Gamma \\ &= 1.3 \times 10^{17} \mathcal{L}_{X,40}^{-3/2} \mathcal{L}_{frb,37}^{3/2} \Delta t_{frb,-3}^{1/10} \xi_{-4}^{-7/5} \sigma_0^{1/2} \epsilon_{e,-1}^2 H(26)\end{aligned}$$

$$\begin{aligned}\nu_c &= \frac{3eB'_{sh}}{4\pi m_e c} \gamma_c^2 \Gamma \\ &= 1.5 \times 10^{18} \mathcal{L}_{X,40}^{1/2} \mathcal{L}_{frb,37}^{-1/2} \Delta t_{frb,-3}^{1/2} \xi_{-4}^{-3/2} t_{-3}^{-2} H(27)\end{aligned}$$

and the peak chromatic luminosity at the peak frequency  $\min(\nu_m, \nu_c)$

$$\begin{aligned}L_{\nu, \max}^{\text{syn}} &= N_{e,sh} \frac{m_e c^2 \sigma_T}{3e} B'_{sh} \Gamma \\ &= 3.9 \times 10^{20} \mathcal{L}_{X,40}^{3/2} \mathcal{L}_{frb,37}^{-1/2} \Delta t_{frb,-3}^{-3/10} \\ &\quad \times \xi_{-4}^{1/5} \sigma_0^{1/2} t_{-3} \text{erg s}^{-1} \text{Hz}^{-1},\end{aligned}\quad (28)$$

where  $\gamma_m = \epsilon_e \Gamma(m_p/m_e)(p-2)/(p-1)$ ,  $\gamma_c = 6\pi m_e c / (\sigma_T B'_{sh} \Gamma t)$ ,  $B'_{sh} = \sqrt{8\pi \sigma e'_{sh}}$ , and the total number of the shocked electrons is given by  $N_{e,sh} = 2\Gamma^2 c t \Sigma_{\pm} n_c$ . The parameters  $\epsilon_e$  and  $p$  are introduced to describe the energy fraction and the distribution index of the shocked electrons. The dynamical time  $t$  of the shock is on the order of a millisecond, by considering that the  $e^{\pm}$  ejecta has a millisecond duration. For the adopted parameter values, the shocked electrons in the slow cooling state can determine a luminosity of

$$\begin{aligned}L_X^{\text{syn}} &= \nu_c L_{\nu, \max}^{\text{syn}} \left( \frac{\nu_c}{\nu_m} \right)^{-(p-1)/2} \\ &= 1.2 \times 10^{38} \mathcal{L}_{X,40}^{(3-p)} \mathcal{L}_{frb,37}^{p-2} \Delta t_{frb,-3}^{(2-p)/5} \\ &\quad \times \xi_{-4}^{6(2-p)/5} \epsilon_{e,-1}^{p-1} \sigma_0^{p-2} t_{-3}^{p-2} \text{erg s}^{-1} \text{cm}^{-2} \text{erg s}^{-1}\end{aligned}\quad (29)$$

which seems much smaller than the isotropic luminosity of the original XRB. However, by considering of the relativistic beaming of the shock emission, the observed flux of this synchrotron X-ray emission can actually reach to be as high as

$$\begin{aligned}F_X^{\text{syn}} &= \frac{\Gamma^2 L_X^{\text{syn}}}{4\pi d^2} \\ &= 2.4 \times 10^{-6} \mathcal{L}_{X,40}^{2-p} \mathcal{L}_{frb,37}^{p-1} \Delta t_{frb,-3}^{(3-p)/5} \\ &\quad \times \xi_{-4}^{2(4-3p)/5} \epsilon_{e,-1}^{p-1} \sigma_0^{p-2} t_{-3}^{p-2} \text{erg s}^{-1} \text{cm}^{-2},\end{aligned}\quad (30)$$

which is even several times higher than the flux of the original XRB. This intense millisecond X-ray pulse overlapping the XRB emission provides an observational signature of the shock-powered SM model, although it could be not very easy to be identified from the X-ray observations because of its short duration. In any case, it is indicated that the value of  $\xi$  cannot be much smaller than  $10^{-4}$ , otherwise this synchrotron X-ray pulse would become too significant to be consistent with the current observation.

#### 4. CONCLUSION AND DISCUSSIONS

The discovery of FRB 200428 from the Galactic magnetar SGRB 1935+2154 during its active state robustly

indicated that the FRB phenomena can be produced by magnetars and, more specifically, be powered by the burst activities. However, it is uncertain whether this indication is also available for the cosmological FRBs. This Letter is devoted to test the applicability of the shock-powered SM model in accounting for this FRB-XRB association event. It is found that the model can in principle survive, if the parameter constraints presented in Equations (18), (19), (20), (24), and (25) can be satisfied. To be specific, a burst ejecta should include an ultra-relativistic  $e^{\pm}$  component of a Lorentz factor of several thousands and a subrelativistic baryonic component of a velocity of  $\sim 0.1c$ . Furthermore, it is required that the highly magnetized  $e^{\pm}$  component should be highly collimated, e.g., has a cross section of  $\sim 10^{21} \text{cm}^2$  at a distance of  $\sim 10^{14} \text{cm}$  from the magnetar. It looks like a cylindrical jet. On the contrary, the baryonic component is probably much spreading and magnetized with a degree of  $\sigma \sim 1.0$ . Under these conditions, the peak frequency of the SM radiation  $\nu_{\text{pk}}$  could be determined to be about a few hundred MHz, with a radiation efficiency of  $\xi \sim 10^{-4}$ .

In view of the high collimation of the  $e^{\pm}$  ejecta and the relativistic beaming of the radiation, the FRB-XRB association can be discovered only on-axis. Therefore, most XRBs would not be detected to accompany with an FRB, just as constrained by the FAST observations (Lin et al. 2020). If observed off-axis, a relatively long time delay appears between the FRB and the magnetosphere XRB. Furthermore, the FRB emission can be significantly reduced by the relativistic beaming effect. Nevertheless, if the deviating angle of the collision from the LOS is not too large (e.g.,  $\Gamma^{-1} \lesssim \theta_v \ll 1$ ), a relatively weak FRB could still be detected. The corresponding time delay can be given by  $\Delta t_{\text{frb}} \sim R_{\text{frb}} \theta_v^2 / (2c)$ , which makes it not easy to find out the FRB-XRB association. The relatively faint radio pulse detected by FAST on 30 April (Zhang et al. 2020a) could just be in such a case. Additionally, of course, we cannot rule out that this faint radio pulse could in fact belong to the pulsation radio emission of the magnetar.

The model-predicted synchrotron X-ray emission can in principle provide a signature to test the shock-powered SM model. However, as another possibility, it cannot be ruled out that, maybe, the observed XRB emission itself is actually just contributed by this shock synchrotron emission (Margalit et al. 2020), rather than being produced in the magnetosphere. Nevertheless, in order to account for the different temporal behaviors of the FRB and XRB, it is required that the shock can at least last for a time much longer than the deceleration timescale (Metzger et al. 2019). The material blocking the  $e^{\pm}$  ejecta should be wind-like rather than shell-like, although it is unclear how can such a wind-like environment be formed. In this case, the analyses and calculations presented in this Letter need to be somewhat modified, but the parameter constraints given in Equations (18), (19), and (20) would not be changed significantly.

The physical processes described in this Letter make this Galactic FRB somewhat similar to type III solar radio bursts, which can also be associated with some X-ray flares (Pick & Vilmer 2008) and can be accounted for by an energy transfer from an electron beam to the ambient medium (Reid & Ratcliffe 2014). Additionally, such a

similarity between FRBs and solar radio bursts had also been found by a statistical study for the cosmological repeating FRBs by Zhang et al. (2019).

The authors thank Bing Zhang for useful discussions.

## REFERENCES

Bannister, K. W., Shannon, R. M., Macquart, J.-P., et al. 2017, *ApJL*, 841, L12

Barthelmy, S. D., Bernardini, M. G., D'Avanzo, P., Groppi, J. D., Kennea, J. A., Lien, A. Y., Melandri, A., Palmer, D. M., Sbarato, T., and Siegel, M. H. on behalf of the Neil Gehrels Swift Observatory Team, 2020, *GCN* #27657

Beloborodov, A. M. 2017, *ApJ*, 843, L26

Burke-Spolaor, S., & Bannister, K. W. 2014, *ApJ*, 792, 19

Bochenek, C. D., Ravi, V., Belov, K. V., Hallinan, G., Kocz, J., Kulkarni, S. R., & McKenna, D. L. 2020, arXiv: 2005.10828

Caleb, M., Flynn, C., Bailes, M., et al. 2017, *MNRAS*, 468, 3746

Cao, X.-F., Yu, Y.-W., & Dai, Z.-G. 2017b, *ApJ*, 839, L20

Champion, D. J., Petroff, E., Kramer, M., et al. 2016, *MNRAS*, 460, L30

The CHIME/FRB Collaboration, 2020, arXiv: 2005.10324

Connor, L., Sievers, J., & Pen, U.-L. 2016, *MNRAS*, 458, L19

Cordes, J. M., & Wasserman, I. 2016, *MNRAS*, 457, 232

Dai, Z. G. 2020, arXiv e-prints, arXiv:2005.12048

Dai, Z. G., Wang, J. S., & Yu, Y. W. 2017, *ApJL*, 838, L7

Ghisellini, G. 2017, *MNRAS*, 465, L30

Israel, G. L., Esposito, P., Rea, N., et al. 2016, *MNRAS*, 457, 3448

Kashiyama, K., & Murase, K. 2017, *ApJ*, 839, L3

Katz, J. I. 2016b, *ApJ*, 826, 226

Keane, E. F., Johnston, S., Bhandari, S., et al. 2016, *Nature*, 530, 453

Keane, E. F., Stappers, B. W., Kramer, M., & Lyne, A. G. 2012, *MNRAS*, 425, L71

Kothes et al. 2018, *ApJ*, 852, 54

Kulkarni, S. R., Ofek, E. O.,Neill, J. D., Zheng, Z., & Juric, M. 2014, *ApJ*, 797, 70

Kumar, P., & Lu, W. 2020, *MNRAS*, 494, 1217

Kumar, P., Lu, W., & Bhattacharya, M. 2017, *MNRAS*, 468, 2726

Li, C.K., Lin, L., Xiong, S.L. et al., 2020, arXiv:2005.11071

Lin, L., Zhang, C. F., Wang, P. et al. 2020, arXiv:2005.11479

Long, K., & Pe'er, A. 2018, *ApJ*, 864, L12

Lorimer, D. R., Bailes, M., McLaughlin, M. A., Narkevic, D. J., & Crawford, F. 2007, *Science*, 318, 777

Lu, W. B., & Kumar, P. 2016, *MNRAS*, 461, L122

Lu, W., & Kumar, P. 2018, *MNRAS*, 477, 2470

Lu, W. B., Kumar, P., & Zhang, B. 2020, arXiv: 2005.06736

Lyubarsky, Y. 2014, *MNRAS*, 442, L9

Lyubarsky, Y., & Ostrovska, S. 2016, *ApJ*, 818, 74

Lyutikov, M. 2017, *ApJ*, 838, L13

Margalit, B., Beniamini, P., Sridhar, N., & Metzger, B. D. 2020, arXiv: 2005.05283

Masui, K., Lin, H.-H., Sievers, J., et al. 2015, *Nature*, 528, 523

Mereghetti, S., Savchenko, V., Ferrigno, C., et al. 2020, arXiv e-prints, arXiv:2005.06335

Metzger, B. D., Berger, E., & Margalit, B. 2017, *ApJ*, 841, 14

Metzger, B. D., Margalit, B., & Sironi, L. 2019, *MNRAS*, 485, 4091

Michilli, D., Seymour, A., Hessels, J. W. T., et al. 2018, *Nature*, 553, 182

Pearlman, A. B., Majid, W. A., Prince, T. A., et al. 2020, arXiv e-prints, arXiv:2005.08410

Petroff, E., Burke-Spolaor, S., Keane, E. F., et al. 2017, *MNRAS*, 469, 4465

Pick, M., & Vilmer, N. 2008, *A&A Rev.*, 16, 1

Plotnikov, I., & Sironi, L. 2019, *MNRAS*, 485, 3816

Popov, S. B., & Postnov, K. A. 2010, *Evolution of Cosmic Objects through their Physical Activity*, 129

Ravi, V., Shannon, R. M., & Jameson, A. 2015, *ApJ*, 799, L5

Reid, H. A. S., & Ratcliffe, H. 2014, *Research in Astronomy and Astrophysics*, 14, 773

Ridnaia, A., Golenetskii, S., Aptekar, R., Frederiks, D., Ulanov, M., Svinkin, D., Tsvetkova, A., Lysenko, A., and Cline, T. on behalf of the Konus-Wind team, 2020, *GCN* #27554

Ridnaia, A., Golenetskii, S., Aptekar, R., Frederiks, D., Ulanov, M., Svinkin, D., Tsvetkova, A., Lysenko, A., and Cline, T. 2020, *ATEL* #13688

Spitler, L. G., Cordes, J. M., Hessels, J. W. T., et al. 2014, *ApJ*, 790, 101

Palmer, D. M. on behalf of the Swift/BAT Team, 2020, *ATEL* #13685

Tavani, M., Casentini, C., Ursi1, A., et al. 2020, arXiv: 2005.12164

Thornton, D., Stappers, B., Bailes, M., et al. 2013, *Science*, 341, 53

Veres, P., Bissaldi, E., and Briggs, M. S. on behalf of the Fermi GBM Team, 2020, *GCN* #27531

Wang, W., Zhang, B., Chen, X., et al. 2019, *ApJ*, 876, L15

Waxman, E. 2017, *ApJ*, 842, 34

Yang, Y.-P., & Zhang, B. 2020, *ApJ*, 892, L10

Yang, Y.-P., & Zhang, B. 2018, *ApJ*, 868, 31

Zhang, G. Q., Wang, F. Y., & Dai, Z. G. 2019, arXiv e-prints, arXiv:1903.11895

Zhang, C. F., Jiang, J. C., Men, Y. P., et al. 2020, *ATel* #13699

Zhong, S. Q., Dai, Z. G., Zhang, H. M., Deng, C. M. 2020, arXiv: 2005.11109

Zhou, P., Zhou, X., Chen, Y., Wang, J. S., Vink, J., & Wang, Y. 2020, arXiv: 2005.03517

This work is supported by the National Natural Science Foundation of China (Grant Nos. 11822302 and 11833003) and the Fundamental Research Funds for the Central Universities (Grant No. CCNU18ZDPY06).